Fizika Nizkikh Temperatur, 2010, v. 36, Nos. 10/11, p. 1253–1263

Exact analytical solution of a classical problem of the Josephson tunnel junction

S.V. Kuplevakhsky and A.M. Glukhov

B.I. Verkin Institute for Low Temperature Physics and Engineering of the National Academy of Sciences of Ukraine
47 Lenin Ave., 61103 Kharkov, Ukraine
E-mail: kuplevakhsky@ilt.kharkov.ua

Received April 30, 2010

We present the exact and complete analytical solution of the classical problem of the Josephson tunnel junction of arbitrary length $W \in (0, \infty)$ in the presence of externally applied magnetic fields and transport currents. Contrary to a wide-spread belief, the exact analytical solution unambiguously proves the absence of any *qualitative* difference between the so-called «small» ($W << 1$) and «large» junctions ($W >> 1$). Another unexpected physical implication of the exact analytical solution is the existence (in the current-carrying state) of *unquantized* Josephson vortices carrying fractional flux and located near one of the junction's edges. We also refine on the mathematical definition of critical transport current.

PACS: **74.50.+r** Tunneling phenomena; Josephson effects;
03.75.Lm Tunneling, Josephson effect, Bose–Einstein condensates in periodic potentials, solitons, vortices, and topological excitations;
02.30.Oz Bifurcation theory.

Keywords: Josephson tunnel junction, vortex structure, critical current.

1. Introduction

One of Kulik's most cited papers is concerned with certain theoretical aspects of vortex statics and dynamics in superconducting (Josephson) tunnel junctions in the presence of externally applied electromagnetic fields [1]. The problem of the response of these junctions to external electromagnetic fields was originally posed by Josephson himself [2]. However, in spite of considerable contribution by many authors (see, e.g., references in relevant books [3–6], and Refs. 7–9), even a simpler problem of equilibrium properties of Josephson tunnel junctions in the presence of externally applied parallel magnetic fields and transport currents could not find an exact and complete analytical solution until recently [10,11].

In the present paper, we review the exact analytical solution of Refs. 10, 11 and discuss some nontrivial physical implications, such as, e.g., the absence of any qualitative difference between the so-called «small» and «large» junctions and the existence of unquantized Josephson vortices in the current-carrying state. In addition, we clarify a subtle mathematical point concerning the definition of critical transport current (Appendix A).

In Fig. 1, we present schematically the geometry of the problem. Here, the x axis is perpendicular to the insulating layer I (the barrier) between two identical superconductors S; the y axis is along the barrier whose length is $W = 2L \in (0, \infty)$. A constant, homogeneous external magnetic field $\mathbf{H}$ is applied along the axis z: $\mathbf{H} = (0, 0, H \geq 0)$. Full homogeneity along the z axis is assumed. The transport current $\mathbf{J}$ is injected along the axis x: $\mathbf{J} = (J, 0, 0)$.

In the region of field penetration, the electrodynamics of the junction in equilibrium is fully described by a time-independent phase difference at the barrier, $\phi = \phi(y)$. The local magnetic field $\mathbf{h} = (0, 0, h)$ and the tunneling current density $\mathbf{j} = (j, 0, 0)$ are given by the Josephson relations [2]

$$h = \frac{1}{2ed}\frac{d\phi}{dy} \quad (\hbar = c = 1), \tag{1}$$

$$j = j_0 \sin\phi. \tag{2}$$

Combining relations (1), (2) and the Maxwell equation $\nabla \times \mathbf{h} = 4\pi\mathbf{j}$, we get [12]

$$\frac{d^2\phi}{dy^2} = \frac{1}{\lambda_J^2}\sin\phi, \tag{3}$$

where $\lambda_J \equiv (8\pi e d j_0)^{-1/2}$ (Josephson penetration depth). (Note this well-known equation [13] can be regarded as the static form of the time-dependent sine-Gordon (SG) equation [14,15].) Appropriate physical boundary conditions are given by [16,17]

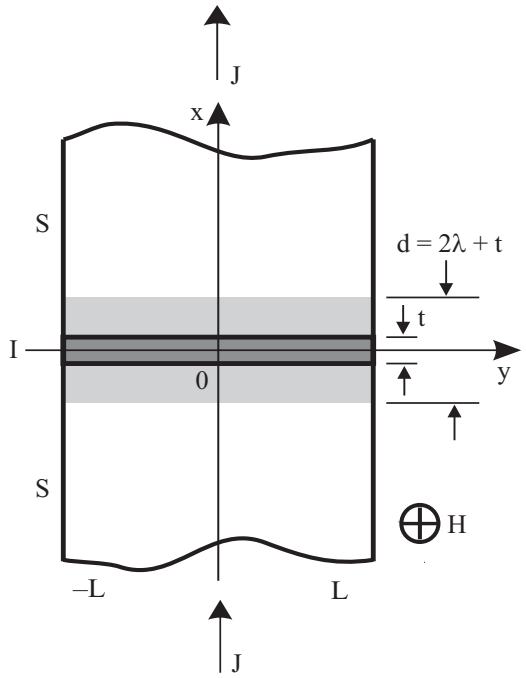

Fig. 1. The geometry of the problem: t is the thickness of the barrier; $W = 2L$ is the length of the barrier; λ is the London penetration depth; $d = 2\lambda + t$ is the width of the field-penetration region (shaded). The external magnetic field **H** is directed into the plane of the figure, and the transport current **J** is along the axis x.

$$H = \frac{1}{4ed}\left[\frac{d\phi}{dy}(L) + \frac{d\phi}{dy}(-L)\right], \tag{4}$$

$$J = \frac{1}{8\pi ed}\left[\frac{d\phi}{dy}(L) - \frac{d\phi}{dy}(-L)\right], \tag{5}$$

where

$$J = \int_{-L}^{L} dy\; j(y) \tag{6}$$

is the transport current per unit length along the z axis. [Boundary conditions (4), (5) correspond to symmetric (with respect to the plane (y,z)) injection of the transport current. More general boundary conditions (allowing for asymmetric injection of J) are considered in Ref. 11.]

Although the SG equation (3) admits straightforward integration [13], the constants of integration specifying particular physical solutions cannot be determined directly from boundary conditions (4), (5). (For $J = 0$, this fact was pointed out in the book by Kulik and Yanson [3].) Mathematically, the reason lies in ill-posedness [18] of the nonlinear boundary-value problem (3)–(5). Indeed: (i) for $|J|$ larger than certain $J_{\max} = J_{\max}(H, L)$, the problem (3)–(5) does not admit any solutions at all; (ii) aside from stable (physical) solutions, there may exist unstable (unphysical) solutions for the same H and J; (iii) for the same H and J, there may exist several different physical solutions.

A comprehensive analysis of attempts in previous literature to overcome the above-mentioned difficulty is given in Ref. 10 ($H \neq 0$, $J = 0$) and Ref. 11 ($H \neq 0$, $J \neq 0$). As to the approach of Refs. 10, 11 itself, it is based on ideas of the theory of stability [19,20]. Within the framework of this approach, for instance, the most important physical quantity, critical transport current $J_c = J_c(H)$, appears quite naturally as the boundary of stability regions of current-carrying states [21]. Mathematical methods developed in Refs. 10, 11 allowed the authors to derive the complete set of particular solutions to (3)–(5) along with the complete set of exact functional equations that uniquely determine corresponding stability regions: see the main text of the present paper for more detail.

In Sec. 2, we provide a necessary mathematical background. In Sec. 3, the exact analytical solution is derived. Section 4 is concerned with a discussion of major physical implications of the exact solution. In Sec. 5, we summarize the obtained results and make several concluding remarks. Finally, in Appendix A, we prove the important identity $J_c \equiv J_{\max}$ [21], which establishes a relationship to the procedure of numerical maximization of J employed in previous literature [17].

2. Mathematical background

2.1. Dimensionless units

From now on, we will employ dimensionless units. Thus, the length scale along the y axis is normalized to the Josephson penetration depth λ_J. The magnetic field is normalized to the superheating field of the Meissner state in a semi-infinite junction [3] $H_s = (ed\lambda_J)^{-1}$. The energy scale is normalized to $d\lambda_J H_s^2/16$. In these dimensionless units, local magnetic field and the Josephson current density are given by

$$h = \frac{1}{2}\frac{d\phi}{dy}, \tag{7}$$

$$j = \frac{1}{2}\sin\phi; \tag{8}$$

the flux quantum is $\Phi_0 = \pi$. Accordingly, the equation for the phase difference and the boundary conditions read

$$\frac{d^2\phi}{dy^2} = \sin\phi, \tag{9}$$

$$H = \frac{1}{4}\left[\frac{d\phi}{dy}(L) + \frac{d\phi}{dy}(-L)\right], \tag{10}$$

$$J = \frac{1}{2}\left[\frac{d\phi}{dy}(L) - \frac{d\phi}{dy}(-L)\right]. \tag{11}$$

2.2. Solution of the static SG equation

Equation (9) has obvious y-independent particular solutions:

$$\phi_n = \pi n,\ n = 0, \pm 1, \ldots$$

Using the first integral,

$$\frac{1}{2}\left[\frac{d\phi}{dy}\right]^2 + \cos\phi = C, \quad -1 \le C < \infty \tag{12}$$

(C is a constant of integration), we obtain the general solution [13]

$$y - y_0 = \pm\frac{1}{\sqrt{2}}\int\frac{d\phi}{\sqrt{C-\cos\phi}} = \begin{cases} \pm F\left(\arcsin\left(\dfrac{1}{k}\cos\dfrac{\phi}{2}\right), k\right), & k \equiv \dfrac{1+C}{2},\ |C|<1,\ \arccos C < |\phi| < \pi; & (13) \\ \pm kF\left(\dfrac{\phi+\pi}{2}, k\right), & k \equiv \dfrac{2}{1+C},\ 1 < C < \infty; & (14) \\ \pm \ln\tan\left(\dfrac{\phi}{4}\right), & C = 1, & (15) \end{cases}$$

where y_0 is the second constant of integration, and $F(\varphi, k)$ is an elliptic integral of the first kind [22].

Note that solution (13) is bounded [in the sense that $|\phi(L) - \phi(-L)| < 2\pi$], whereas solution (14) is not. Solution (15) is the limiting case of solutions (13) and (14) for $C \to 1 \mp 0$, respectively.

2.3. Analysis of stability

Our analysis of stability is based on a minimization procedure for the generating Gibbs free-energy functional taken per unit length along the z axis:

$$\Omega_G\left[\phi, \frac{d\phi}{dy}; H, J\right] = 2H^2 W + \int_{-L}^{L} dy\left[1 - \cos\phi(y) + \frac{1}{2}\left[\frac{d\phi(y)}{dy}\right]^2\right] -$$

$$-(2H + J)\phi(L) + (2H - J)\phi(-L). \tag{16}$$

The stationarity condition, $\delta\Omega_G = 0$ ($\delta\Omega_G$ is the first variation of Ω_G), yields the equation for the phase difference (9) and boundary conditions (10), (11).

As shown in Refs. 10, 11, all stationary points of (16) [solutions to (9) under (10), (11)] are either minima (stable, physically observable solutions) or saddle points (absolutely unstable, physically unobservable solutions). The type of a given solution $\phi = \phi(y)$ (determined by the sign of the second variation $\delta\Omega_G^2$) can be established [10,11] by evaluating the lowest eigenvalue $\mu = \mu_0$ of the Sturm–Liouville problem:

$$-\frac{d^2\psi}{dy^2} + \cos\phi(y)\psi = \mu\psi, \quad y \in (-L, L),$$

$$\frac{d\psi}{dy}(\pm L) = 0.$$

Namely, if $\mu_0 < 0$, the solution $\phi = \phi(y)$ corresponds to a saddle point of (16) ($\delta\Omega_G^2 \gtrless 0$), whereas stable physical solutions that minimize (16) are characterized by $\mu_0 > 0$ ($\delta\Omega_G^2 > 0$).

The boundaries of the stability regions for physical solutions ($\delta\Omega_G^2 \ge 0$) are determined by the condition $\mu_0 = 0$, or, equivalently, by the solution $\bar{\psi}_0 = \bar{\psi}_0(y)$ to the boundary-value problem

$$-\frac{d^2\bar{\psi}_0}{dy^2} + \cos\phi(y)\bar{\psi}_0 = 0, \quad y \in (-L, L), \tag{17}$$

$$\frac{d\bar{\psi}_0}{dy}(\pm L) = 0, \tag{18}$$

$$\bar{\psi}_0(y) \ne 0, \quad y \in [-L, L]. \tag{19}$$

Owing to the fact that the boundary-value problem (17)–(19) admits exact analytical solution, the analysis of stability can be brought up to a closed and exact analytical form.

Indeed, the general solution to (17) can be written as

$$\bar{\psi}_0(y) = C_1\chi_1(y) + C_2\chi_2(y), \tag{20}$$

where

$$\chi_1 = \frac{d\phi}{dy} \tag{21}$$

and

$$\chi_2 = \frac{d\phi}{dy}\int\frac{dy}{(d\phi/dy)^2} \tag{22}$$

are linearly independent solutions to (17), and C_1, C_2 are arbitrary constants. Upon the substitution of (20)–(22) into (18), we arrive at our key equation

$$\frac{d\chi_1}{dy}(L)\frac{d\chi_2}{dy}(-L) = \frac{d\chi_1}{dy}(-L)\frac{d\chi_2}{dy}(L). \tag{23}$$

Equation (23), under condition (19), implicitly determines boundaries of the stability region for any physical solution $\phi = \phi(y)$.

3. The complete set of exact physical solutions

3.1. The case $H \geq 0$, $J \geq 0$

3.1.1. The bounded solution. Relations (13) and (20)–(22) yield

$$\phi_s(y) = 2\arccos\left[k\frac{\mathrm{cn}(y+\beta,k)}{\mathrm{dn}(y+\beta,k)}\right], \quad k \in [k_c,1), \quad \beta \in [0,\beta_c], \tag{24}$$

where $k_c = k_c(L)$ satisfies the functional equation

$$\mathrm{cn}(L,k_c)\left[-E(L,k_c)+\left(1-k_c^2\right)L\right]+ \\ +\left(1-k_c^2\right)\mathrm{sn}(L,k_c)\,\mathrm{dn}(L,k_c) = 0. \tag{25}$$

The boundary of the stability region $\beta_c = \beta_c(k)$ is determined by the solution to the functional equation

$$\mathrm{cn}(L+\beta_c,k)\,\mathrm{cn}(L-\beta_c,k)\times \\ \times\left[-E(L+\beta_c,k)-E(L-\beta_c,k)+2\left(1-k^2\right)L\right]+ \\ +\left(1-k^2\right)\left[\mathrm{sn}(L+\beta_c,k)\,\mathrm{cn}(L-\beta_c,k)\,\mathrm{dn}(L+\beta_c,k)+\right. \\ \left.+\mathrm{sn}(L-\beta_c,k)\,\mathrm{cn}(L+\beta_c,k)\,\mathrm{dn}(L-\beta_c,k)\right] = 0, \quad k \in [k_c,1), \tag{26}$$

under the condition $\beta_c(k_c) = 0$ [$\beta_c \in [0,K(k))$]. Here and in what follows, $K(k)$ is the complete elliptic integral of the first kind, $E(\varphi,k)$ is an elliptic integral of the second kind; $\mathrm{sn}\,u$, $\mathrm{cn}\,u$, $\mathrm{dn}\,u = d\,\mathrm{am}\,u/du$, and $\mathrm{am}\,u$ are Jacobian elliptic functions [22].

3.1.2. Unbounded solutions. Relations (14) and (20)–(22) yield an infinite set of solutions

$$\phi_p(y) = \pi(p-1)+2\mathrm{am}\left(\frac{y}{k}+K(k)+\alpha,k\right), \tag{27}$$

$$\alpha \in [0,\alpha_c],\ p = 2m\ (m = 0,1,\ldots);$$

$$\phi_p(y) = \pi p + 2\mathrm{am}\left(\frac{y}{k}+\alpha,k\right), \tag{28}$$

$$\alpha \in [0,\alpha_c],\ p = 2m+1\ (m = 0,1,\ldots),$$

$$k \in S_p,\ \cup_{p=0}^{\infty} S_p = (0,1),$$

where the regions S_p are defined by the relations

$$S_0 \equiv (k_1,1); \quad S_p \equiv (k_{p+1},k_p],\ p = 1,2,\ldots; \tag{29}$$

$$pk_pK(k_p) = L. \tag{30}$$

The boundaries of the stability regions $\alpha_c = \alpha_c(k)$ are determined by the solutions to the functional equations

$$k^2\mathrm{sn}\left(\frac{L}{k}+\alpha_c,k\right)\mathrm{sn}\left(\frac{L}{k}-\alpha_c,k\right)\mathrm{cn}\left(\frac{L}{k}+\alpha_c,k\right)\mathrm{cn}\left(\frac{L}{k}-\alpha_c,k\right)\left[E\left(\frac{L}{k}+\alpha_c,k\right)+E\left(\frac{L}{k}-\alpha_c,k\right)\right]+ \\ +\mathrm{sn}\left(\frac{L}{k}-\alpha_c,k\right)\mathrm{cn}\left(\frac{L}{k}-\alpha_c,k\right)\mathrm{dn}^3\left(\frac{L}{k}+\alpha_c,k\right)+\mathrm{sn}\left(\frac{L}{k}+\alpha_c,k\right)\mathrm{cn}\left(\frac{L}{k}+\alpha_c,k\right)\mathrm{dn}^3\left(\frac{L}{k}-\alpha_c,k\right) = 0\ (p = 2m); \tag{31}$$

$$\frac{k^2}{1-k^2}\mathrm{sn}\left(\frac{L}{k}+\alpha_c,k\right)\mathrm{sn}\left(\frac{L}{k}-\alpha_c,k\right)\mathrm{cn}\left(\frac{L}{k}+\alpha_c,k\right)\mathrm{cn}\left(\frac{L}{k}-\alpha_c,k\right)\left\{E\left(\frac{L}{k}+\alpha_c,k\right)+\right. \\ \left.+E\left(\frac{L}{k}-\alpha_c,k\right)-k^2\left[\frac{\mathrm{sn}\left(\frac{L}{k}+\alpha_c,k\right)\mathrm{cn}\left(\frac{L}{k}+\alpha_c,k\right)}{\mathrm{dn}\left(\frac{L}{k}+\alpha_c,k\right)}+\frac{\mathrm{sn}\left(\frac{L}{k}-\alpha_c,k\right)\mathrm{cn}\left(\frac{L}{k}-\alpha_c,k\right)}{\mathrm{dn}\left(\frac{L}{k}-\alpha_c,k\right)}\right]\right\}- \\ -\frac{\mathrm{sn}\left(\frac{L}{k}-\alpha_c,k\right)\mathrm{cn}\left(\frac{L}{k}-\alpha_c,k\right)}{\mathrm{dn}\left(\frac{L}{k}+\alpha_c,k\right)}-\frac{\mathrm{sn}\left(\frac{L}{k}+\alpha_c,k\right)\mathrm{cn}\left(\frac{L}{k}+\alpha_c,k\right)}{\mathrm{dn}\left(\frac{L}{k}-\alpha_c,k\right)} = 0 \quad (p = 2m+1), \tag{32}$$

under the conditions $\alpha_c(k_p) = 0$ [$\alpha_c \in [0,K(k))$]. The meaning of the parameter $p = 0, 1, 2,\ldots$ is revealed by the relation

$$p = \left\lfloor \frac{\phi_p(L)-\phi_p(-L)}{2\pi} \right\rfloor, \tag{33}$$

where $\lfloor\ldots\rfloor$ stands for the integer part of the argument: physically, $p > 0$ represent the number of quantized Josephson vortices carrying the flux quantum $\Phi_0 = \pi$, whereas $p = 0$ signifies the Meissner solution.

3.1.3. The limiting solution. Relations (15) and (20)–(22) yield

$$\phi_l(y) = 4\arctan\left[\exp(y-\gamma)\right], \quad \gamma \in [\gamma_c,\infty), \tag{34}$$

where $\gamma_c = \gamma_c(L)$ is determined by the functional equation

$$L\sinh(L-\gamma_c)\sinh(L+\gamma_c) - \frac{1}{2}\sinh^2(L-\gamma_c)\sinh(L+\gamma_c)\cosh(L-\gamma_c) - \frac{1}{2}\sinh^2(L+\gamma_c)\sinh(L-\gamma_c)\cosh(L+\gamma_c) - \sinh(L+\gamma_c)\cosh(L-\gamma_c) - \sinh(L-\gamma_c)\cosh(L+\gamma_c) = 0. \quad (35)$$

Solution (34) is the limiting case of the solutions ϕ_s [Eq. (24)] and ϕ_0 [Eq. (27)] for $k \to 1$.

3.2. Generalization

Physical solutions that do not obey the restrictions $H \geq 0$, $J \geq 0$ are expressed via the solutions ϕ_s [Eq. (24)], ϕ_p [Eqs. (27), (28)] and ϕ_l [Eq. (34)] by means of elementary symmetry relations. Namely,

(1) $H \leq 0$, $J \geq 0$:

$$\phi_s, \beta \to \phi_s, -\beta;\ \phi_p, \alpha \to -\phi_p, -\alpha;\ \phi_l, \gamma \to 2\pi - \phi_l, -\gamma. \quad (36)$$

(2) $H \geq 0$, $J \leq 0$:

$$\phi_s, \beta \to -\phi_s, -\beta;\ \phi_p, \alpha \to \phi_p, -\alpha;\ \phi_l, \gamma \to \phi_l - 2\pi, -\gamma. \quad (37)$$

(3) $H \leq 0$, $J \leq 0$:

$$\phi_s, \beta \to -\phi_s, \beta;\ \phi_p, \alpha \to -\phi_p, \alpha;\ \phi_l, \gamma \to -\phi_l, \gamma. \quad (38)$$

By complementing the formulas of this section with boundary conditions (10) and (11), we obtain a closed set of exact analytical relations for the evaluation of any physical quantity of interest. Major physical implications of this set of solutions are discussed in the next section. Here, we want to emphasize the following: owing to a simple mathematical fact that the derived solutions continuously depend on the parameter $L \equiv W/2$, all the physical properties of junctions with arbitrary $W \in (0, \infty)$ are *qualitatively* the same.

4. Major physical implications

4.1. The Meissner state, vortex structure, and the Gibbs free energy for J = 0

In this case, the complete set of solutions is given by Eqs. (27)–(30) with $\alpha = 0$. They obey the symmetry relation

$$\phi_p(-y) = 2\pi p - \phi_p(y) \quad (39)$$

and the boundary conditions

$$\frac{d\phi_p}{dy}(\pm L) = 2H. \quad (40)$$

Using relations (29), (30) and (40), we derive the stability regions in terms of the field H:

$$p = 0;\quad 0 \leq H < H_0, \quad (41)$$

$$p = 1, 2, \ldots : \sqrt{H_{p-1}^2 - 1} \leq H < H_p, \quad (42)$$

with H_p implicitly determined by

$$(p+1)K\left(\frac{1}{H_p}\right) = H_p L. \quad (43)$$

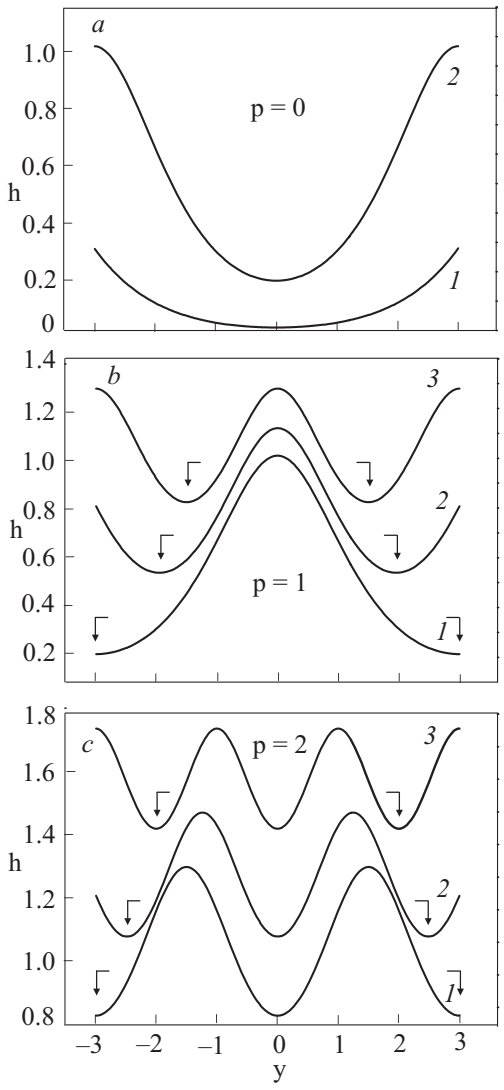

Fig. 2. Spatial distribution of h for $L = 30$. *a* — The Meissner solution ($p = 0$): curves *1* and *2* correspond to the cases $0 < H < H_0$ and $H = H_0$, respectively. *b* — The single-vortex solution ($p = 1$): curves *1–3* correspond to the cases $H = \sqrt{H_0^2 - 1}$, $\sqrt{H_0^2 - 1} < H < H_1$ and $H = H_1$, respectively; the vortex is confined to the spatial interval denoted by bracket-shaped arrows. *c* — The two-vortex solution ($p = 2$): curves *1–3* correspond to the cases $H = \sqrt{H_1^2 - 1}$, $\sqrt{H_1^2 - 1} < H < H_2$ and $H - H_2$, respectively; the vortices are confined to the spatial intervals denoted by bracket-shaped arrows.

Note that each two consecutive stability regions, labeled by p and $p+1$ $(p = 0, 1, 2, \ldots)$, overlap in the field range

$$\sqrt{H_p^2 - 1} \le H < H_p \tag{44}$$

for any $L \in (0, \infty)$. For sufficiently large L, the overlap may involve several consecutive stability regions. In contrast, the overlap decreases with an increase in p and a decrease in L.

Vortex solutions with $p = 1, 2, \ldots$ exist for arbitrary small $W < \infty$, provided the field $H > 0$ is sufficiently high. Josephson vortices themselves are confined to the spatial interval $[-y_p, y_p]$, where y_p is defined by the conditions $\phi(-y_p) = 0$ and $\phi(y_p) = 2\pi p$. The regions of the Meissner effect are $[-L, -y_p)$ and $(y_p, L]$. As an illustration, see Fig. 2, where we plot spatial distribution of the local magnetic field h [Eq. (7)] for the first three solutions $(p = 0, 1, 2)$.

From Eq. (16) with $J = 0$, we obtain exact analytical expressions for the average Gibbs free energy density:

$$\omega(H) \equiv \frac{\Omega_G(H)}{W} = \begin{cases} 2H^2 + \dfrac{8}{W}\left[\dfrac{1}{k}E\left(\dfrac{W}{2k} + K(k), k\right) - \dfrac{1}{k}E(k) - \dfrac{\left(1-k^2\right)W}{4k^2} - H\ \mathrm{am}\left(\dfrac{W}{2k} + K(k), k\right) - \dfrac{\pi}{2}\right], & (45) \\ \qquad k = k(H)\ (p = 2m); & \\ 2H^2 + \dfrac{8}{W}\left[\dfrac{1}{k}E\left(\dfrac{W}{2k}, k\right) - \dfrac{\left(1-k^2\right)W}{4k^2} - H\ \mathrm{am}\left(\dfrac{W}{2k}, k\right)\right], \quad k = k(H)\ (p = 2m+1), & (46) \end{cases}$$

where $E(k)$ is the complete elliptic integrals of the second kind [22].

In Figs. 3,*a* and *b*, we plot $\omega(H)$ for the cases of a «small» $(L = 0.3)$ junction and a «large» $(L = 0.3)$ junction, respectively. Figure 3,*b* exhibits strong overlapping of neighboring states, whereas in Fig. 3,*a* overlapping is practically invisible (see, however, the inset). The envelope of the energy curves for $p = 0, 1, ..., 6$ represents a thermodynamically stable state at a given H. Parts of the energy curves that lie above the envelope in Fig. 3,*b* represent thermodynamically metastable states. For better orientation in the physical situation, we have specified the upper bound of the existence of the Meissner state $(H = H_0)$ and the first thermodynamic critical field [2,3,5] $(H = H_{c1})$. (The latter field is defined by the requirement that the Gibbs free energies of the states $p = 0$ and $p = 1$ be equal to each other.) Both the fields, H_0 and H_{c1}, strongly depend on the length W: they increase (although at different rates) with a decrease of W. For example, for $1 \ll W < \infty$, they are approximately given by $H_0 \approx$ $\approx H_s = 1$ and $H_{c1} \approx 2/\pi$, whereas for $W \ll 1$ they practically coincide: $H_{c1} \approx H_0 \approx \pi/W$ (see Fig. 3,*a*). Note that by decreasing the external field below $H = H_{c1}$, one can still observe the single-vortex state down to the field $H = \sqrt{H_0^2 - 1} < H_{c1}$ (the abscissa of the left end of the energy curve for $p = 1$ in Fig. 3,*b*): thus, hysteresis is inherent in any Josephson junction.

In the limit $H \gg \max(1, W)$ (negligibly small screening by Josephson currents), all the physical quantities can be approximated by elementary functions [23]:

$$\phi_p(y) \approx p\pi + 2Hy - \frac{(-1)^p}{4H^2}\left[\sin(2Hy) - 2Hy\cos(HW)\right], \tag{47}$$

$$p = 0: H \in \left(1, \frac{\pi}{W}\right);\ p = 1, 2, \ldots:\ H \in \left(\frac{p\pi}{W}, \frac{(p+1)\pi}{W}\right);$$

$$h(y) \approx H - \frac{(-1)^p}{4H}\left[\cos(2Hy) - \cos(HW)\right], \tag{48}$$

$$j(y) \approx \frac{(-1)^p}{2}\sin(2Hy), \tag{49}$$

$$\omega(H) \approx 1 - \frac{\left|\sin(HW)\right|}{HW} + \frac{1}{8H^2}\left[\cos^2(HW) + \frac{1}{2}\right]. \tag{50}$$

However, asymptotics (47)–(50) break down near the boundaries of the stability regions (41)–(43), when $H \approx p\pi/W$ $(p = 1, 2, \ldots)$.

4.2. Current-carrying states

4.2.1. The critical current for H = 0. The solution is given by (24), (25) with $\beta = 0$. It obeys the symmetry relation

$$\phi_s(-y) = \phi_s(y) \tag{51}$$

and the boundary condition

$$J = \frac{d\phi_s}{dy}(L) \equiv 2k\sqrt{1-k^2}\,\frac{\mathrm{sn}(L,k)}{\mathrm{dn}(L,k)}. \tag{52}$$

In the limit $L \equiv W/2 \ll 1$, expression (52) reduces to the expected result [2–6]

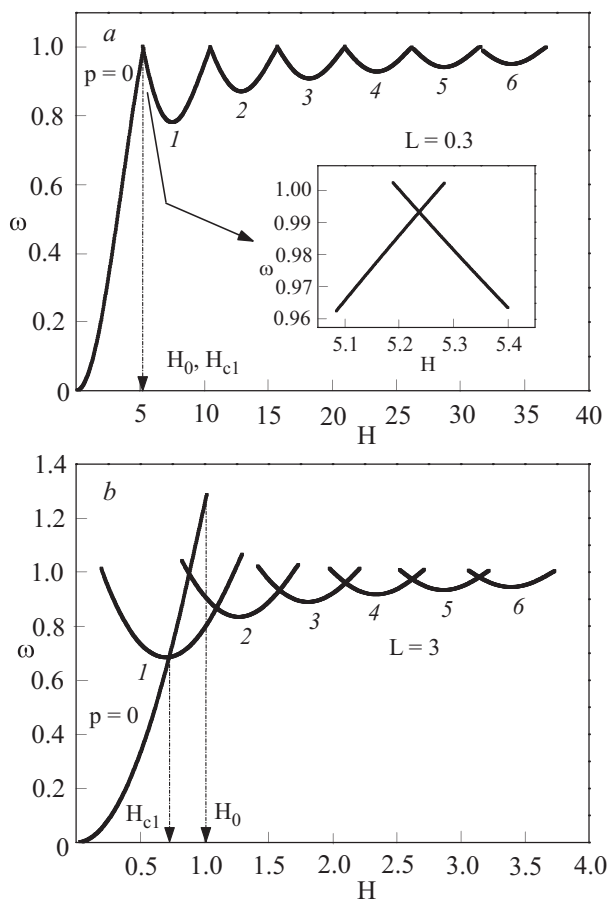

Fig. 3. The average Gibbs free-energy density $\omega(H) \equiv \equiv \Omega_G(H)/W$ for the cases of a «small» ($L = 0.3$) junction (*a*) and a «large» ($L = 3.0$) junction (*b*). Energy curves are shown for $p = 0, 1, \ldots, 6$. The upper bound of the existence of the Meissner state (H_0) and the first thermodynamic critical field (H_{c1}) are also shown.

$$J \approx \frac{W}{2}\sin\phi_s(0), \quad \phi_s(0) = 2\arccos k \in \left[0, \frac{\pi}{2}\right], \quad (53)$$

with $J_c = L$ being the critical current. The dependence $J_c = J_c(L)$ on the whole interval $(0, \infty)$ is plotted in Fig. 4.

4.2.2. The general case, H > 0, J > 0. This case requires the complete set of solutions derived in Sec. 4. Boundary conditions (10) and (11) map the stability regions of these solutions onto the physical plane (*H*, *J*). The boundaries of the stability regions in the physical plane represent the dependence $J_c = J_c(H)$ that consists of an infinite number of separate branches. As an illustration, in Fig. 5, we present the results of this mapping for the first six solutions and $L = 0.3$, 1, 3.

As could be expected, the structure of the stability regions [including the boundaries $J_c = J_c(H)$] is qualitatively the same for all the considered cases: $L = 0.3$ (a «small» junction), $L = 1$ (a «medium» junction), and

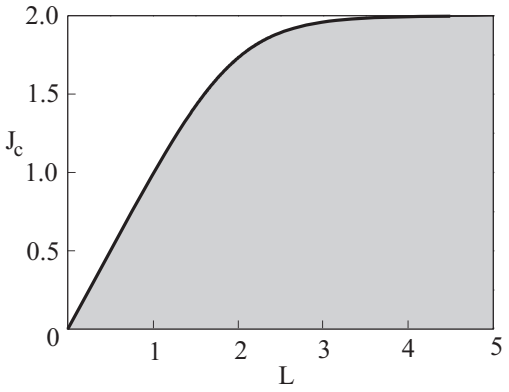

Fig. 4. The dependence $J_c = J_c(L)$ for $H = 0$ (solid line). The region of the existence of current-carrying states is shaded.

$L = 3$ (a «large» junction). Thus, as the solutions ϕ_s [Eq. (24)] and ϕ_0 [Eq. (27)] constitute two different branches of the same current-carrying solution, their stability regions (labeled by the indices s and $p = 0$, respectively) merge to form a unified stability domain. The transformation $\phi_s \leftrightarrow \phi_0$ occurs on an internal boundary (represented by the dashed line in Fig. 5), where these two solutions coincide with the elementary solution ϕ_l [Eq. (34)].

It should be emphasized that the overlap of the stability regions in the physical plane results in multivaluedness of the dependence $J_c = J_c(H)$ for any $W \in (0, \infty)$. It also implies that the critical current J_c does not vanish at any $H > 0$ even for $W \ll 1$.

For $H \gg \max(1, W)$, , the following approximations to the exact analytical solutions can be derived

$$\phi_p(y) \approx p\pi + 2Hy + 2\alpha - \frac{\alpha}{2H^2} - \frac{(-1)^p}{4H^2}[\sin(2Hy + 2\alpha) - 2Hy\cos(HW)\cos(2\alpha)], \quad (54)$$

$$\alpha \in \left[0, \frac{\pi}{4}\right]; \quad p = 0: \quad H \in \left(1, \frac{\pi}{W}\right);$$

$$p = 1, 2, \ldots: \quad H \in \left(\frac{p\pi}{W}, \frac{(p+1)\pi}{W}\right);$$

$$J \approx \frac{1}{2H}\left|\sin(HW)\right|\sin(2\alpha), \quad (55)$$

$$J_c(H) \approx \frac{1}{2H}\left|\sin(HW)\right|. \quad (56)$$

As is the case of (47)–(50), asymptotic expressions (54)–(56) are invalid at $H \approx p\pi/W$ ($p = 1, 2, \ldots$). Thus, expression (56) (known in literature [2,4–6] as «Fraunhofer pattern» of the critical current) does not reveal important features resulting from the overlap of the stability regions (see above), and in the field range $0 < H \lesssim 1$ it can be regarded, at most, as a reasonable interpolation.

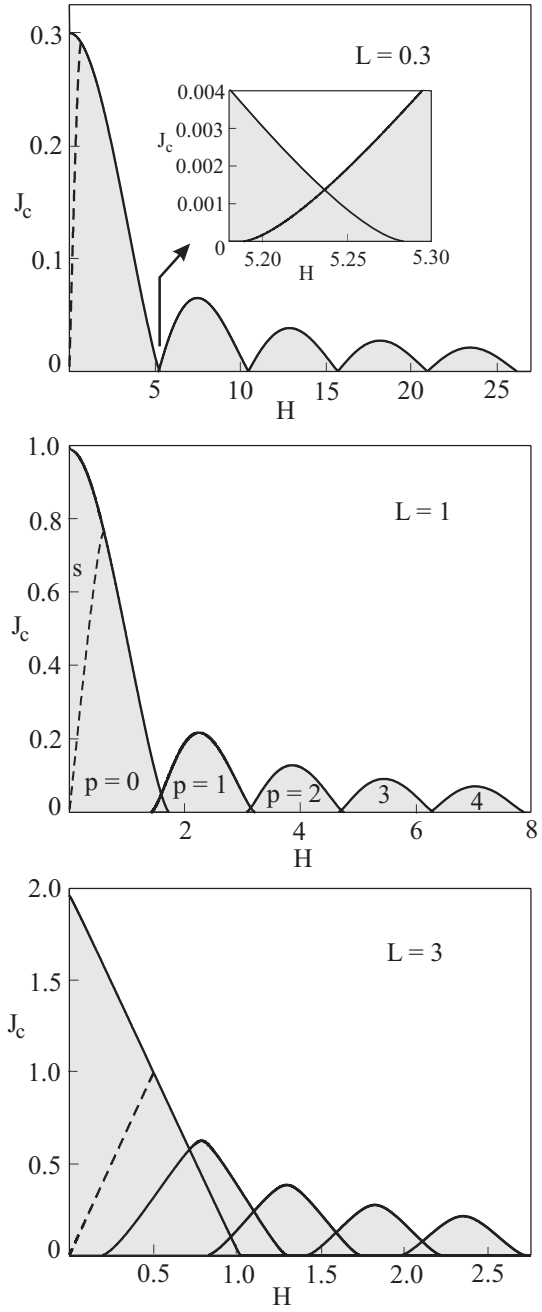

Fig. 5. The regions of the existence of the current-carrying states ϕ_s and ϕ_p $(p = 0, \ldots, 4)$ in the physical plane (H,J) (shaded) for $L = 0.3, 1, 3$. The dependence $J_c = J_c(H)$ is given by the solid lines. The dashed line represents the internal boundary where $\phi_s = \phi_0 = \phi_l$.

4.3. Unquantized Josephson vortices

The exact current-carrying solutions ϕ_p (27)–(28) reveal yet another unexpected physical property: namely, the existence of *unquantized* Josephson vortices carrying flux $\Phi \in \left(\frac{1}{2}\Phi_0, \Phi_0\right)$. Such vortices exist for transport currents

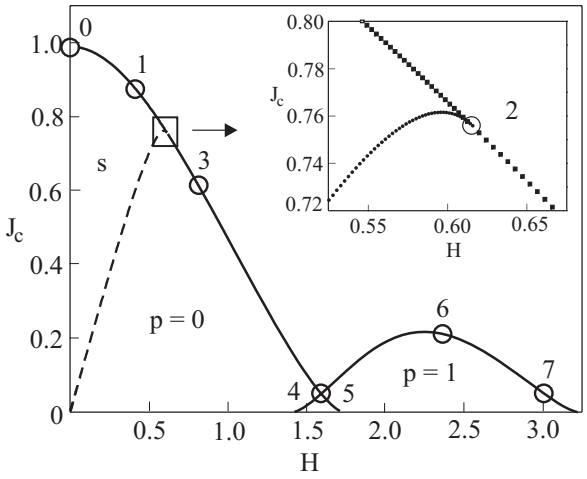

Fig. 6. The first two critical curves $J_c = J_c(H)$ for $L = 1$. Spatial distribution of h and j (Fig. 7) is evaluated at typical points 0–7: (0) $H = 0.00$, $J_c = 0.99$; (1) $H = 0.43$, $J_c = 0.87$; (2) $H = 0.61$, $J_c = 0.76$ $(\phi_s = \phi_0 = \phi_l)$; (3) $H = H_0^* = 0.81$, $J_c = (2H_0^*)^{-1} = 0.61$; (4) $H = 1.60$, $J_c = 0.05$ (the first curve); (5) $H = 1.60$, $J_c = 0.05$ (the second curve); (6) $H = H_1^* = 2.36$, $J_c = (2H_1^*) = 0.21$; (7) $H = 3.01$, $J_c = 0.05$.

close to J_c and are localized near the junction's boundaries $y = \pm L$. Their localization depends on the value of the applied field H.

To be more specific, we note that there exist such field values $H = H_p^*$ $(p = 0,1,2,\ldots)$ that $J_c = (2H_p^*)^{-1}$: they are defined by the relations

$$H_p^* = \frac{1}{2k_p^*}\left[1 + \sqrt{1-(k_p^*)^2}\right], \tag{57}$$

$$\left(p + \frac{1}{2}\right) k_p^* K(k_p^*) = L. \tag{58}$$

For $H < H_p^*$ $(p = 1,2,3,\ldots)$ and $J = J_c$, a single unquantized vortex is located near the junction's boundary $y = -L$, whereas for $H > H_p^*$ $(p = 0,1,2,\ldots)$ and $J = J_c$, such a vortex is located near the boundary $y = L$. At $H = H_p^*$ $(p = 0,1,2,\ldots)$ and $J = J_c$, there are no unquantized vortices in the junction.

This general situation is illustrated in Figs. 6 and 7. For simplicity, in Fig. 6, we restrict ourselves to the first two critical curves $J_c = J_c(H)$ of the junction with $L = 1$. Spatial distribution of h and j at typical points 0–7 on these curves is presented in Fig. 7, were we also mark the locations of both quantized and unquantized Josephson vortices.

In conclusion, we observe that solutions with «unquantized Josephson vortices» formally appear in the case $H \neq 0$, $J = 0$ as well: see Fig. 4 in Ref. 10. However, they prove to be absolutely unstable.

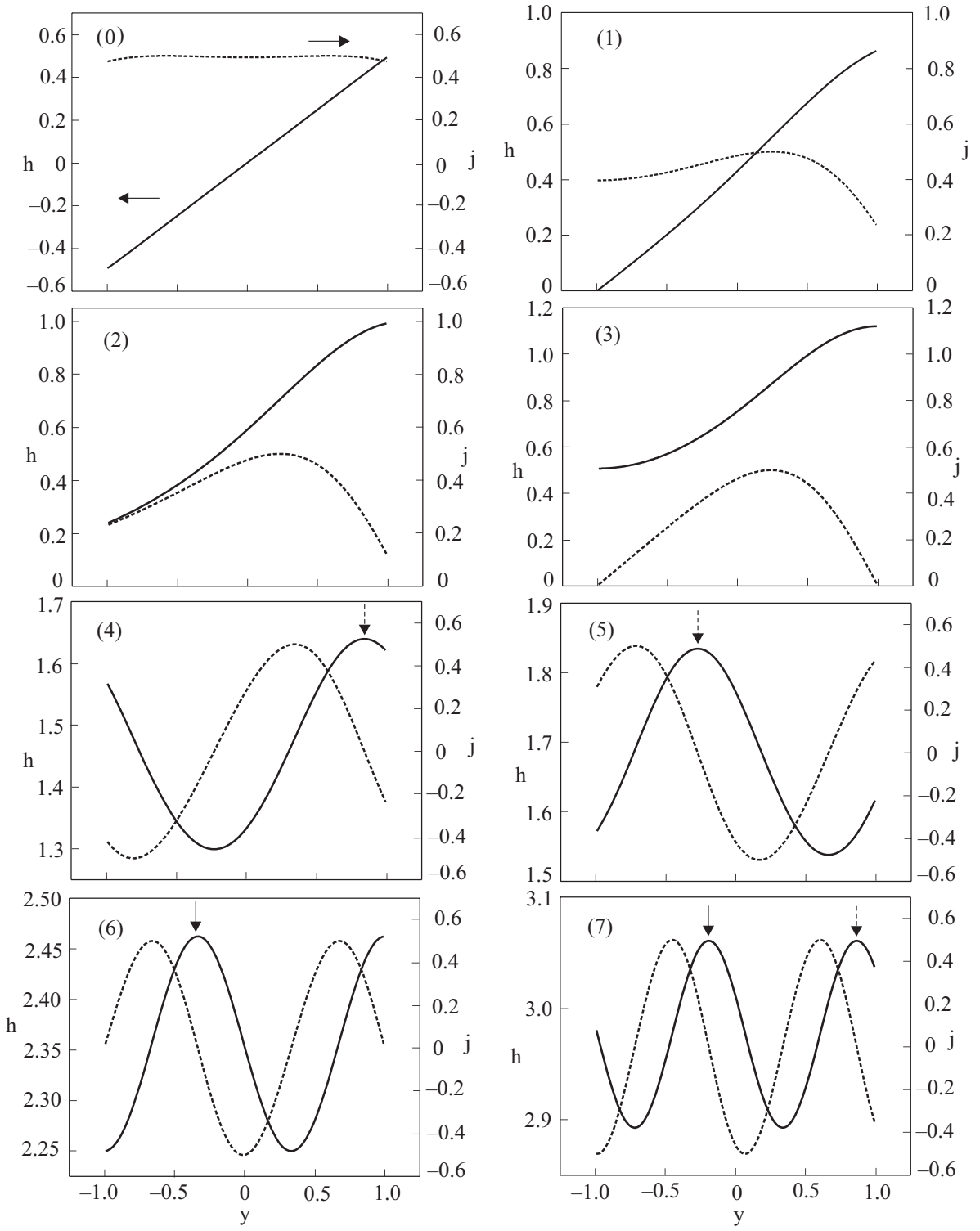

Fig. 7. Spatial distribution of h (solid line) and j (dashed line) for points 0–7 in Fig. 5. The location of Josephson vortices is marked by vertical arrows: the dashed arrows correspond to unquantized vortices ((4), (5) and (7)); the solid arrows correspond to quantized vortices ((6) and (7)).

5. Summary and conclusions

Summarizing, we have obtained the complete and exact physical solution of the classical problem (3)–(5) describing the Josephson tunnel junction of arbitrary length $W \in (0, \infty)$ in the presence of parallel magnetic field H and transport current J. As could be anticipated, the exact analytical solution reveals some nontrivial and even unexpected physical features.

Thus, contrary to a wide-spread belief, our solution unambiguously proves that there is no *qualitative* difference

between the so-called «small» ($W \ll 1$) and «large» junctions ($W \gg 1$). In particular, the multivaluedness of the dependence $J_c = J_c(H)$, as well as hysteresis, are intrinsic features of *any* Josephson junction with $W \in (0, \infty)$.

The existence of *unquantized* Josephson vortices in the current-carrying state of classical Josephson junctions is yet another unexpected feature. This finding should be contrasted with recent theoretical predictions of unquantized vortices (including Josephson ones) in unconventional superconductors [24,25].

We have refined on the mathematical definition of critical transport current (Appendix A). Finally, given that the nonlinear sine-Gordon equation (see Introduction) finds a lot of applications in condensed-matter and elementary-particle physics [14,15], we hope that our exact analytical solution for a static case may find applications outside the field of superconductivity as well.

Acknowledgments

The authors thank A.N. Omelyanchouk and A.S. Kovalev for stimulating discussions.

Appendix A: A proof of the identity $J_c \equiv J_{\max}$

As a prerequisite, we begin by establishing an important fact concerning the derivatives of the general solution (13)–(15) with respect to the constants of integration y_0 and C. For brevity, we denote this solution as

$$\phi = \phi(y + y_0; C) \tag{A.1}$$

and introduce the following notation:

$$\frac{\partial \phi}{\partial y} \equiv \phi'_y, \quad \frac{\partial^2 \phi}{\partial y^2} \equiv \phi''_{yy}, \quad \frac{\partial \phi}{\partial y_0} \equiv \phi'_{y_0}, \quad \frac{\partial^2 \phi}{\partial y \partial y_0} \equiv \phi''_{y_0 y}, \quad \ldots \tag{A.2}$$

The solution ϕ satisfies Eq. (9), whereas ϕ'_{y_0} and ϕ'_C satisfy Eq. (17). Moreover, from (A.1), we immediately find

$$\phi'_{y_0} = \phi'_y \equiv \chi_1. \tag{A.3}$$

Substitution of (A.1) into (12) makes the latter an identity. Differentiating this identity with respect to C, using (A.3) and Eq. (9), we obtain

$$\begin{vmatrix} \phi'_{y_0} & \phi'_C \\ \phi''_{y_0 y} & \phi''_{Cy} \end{vmatrix} = 1,$$

which means that ϕ'_{y_0} and ϕ'_C are linearly independent solutions to (17). Taking into account (A.3), we infer

$$\phi'_C = \text{const}\, \chi_2, \tag{A.4}$$

where χ_2 is given by (22). Now, we can proceed with the proof that $J_c \equiv J_{\max}$.

(1) The case $H = 0$, $J > 0$

Let us rewrite boundary condition (52) on ϕ'_{sy} ($\beta = 0$) as

$$J - \mathcal{J}(L; k) = 0. \tag{A.5}$$

Equation (A.5) defines the dependence $J = J(L)$ for a family of curves parameterized by k. We argue that this family has an *envelope* [26] $J_{\max} = J_{\max}(L)$ that coincides with the curve $J_c = J_c(L)$.

Indeed, the envelope must satisfy (A.5) along with the condition $\mathcal{J}'_k(L; k) = 0$. However, by (A.4), this condition is nothing but $\chi'_{2y}(L; k) = 0$, i.e., functional equation (25) that defines the dependence $k_c = k_c(L)$. This fact is sufficient to argue that $J_c \equiv J_{\max}$.

(2) The case $H > 0$, $J > 0$

Analogously to the previous case, we rewrite boundary conditions (10), (11) on ϕ'_{sy} and ϕ'_{py} ($p = 0, 1, \ldots$) as

$$H - \mathcal{H}(k, \beta) = 0, \quad J - \mathcal{J}(k, \beta) = 0 \tag{A.6}$$

and

$$H - \mathcal{H}(\alpha, k) = 0, \quad J - \mathcal{J}(\alpha, k) = 0, \tag{A.7}$$

respectively. Equations (A.6) for ϕ_s implicitly define the dependence $J = J(H)$ for a family of curves parameterized by β, with k being a parameter along each curve. The same is true of Eqs. (A.7) for ϕ_p, except for the fact that now k parameterizes the family, and α is along each curve. We argue that these families of curves have envelopes $J_{\max} = J_{\max}(L)$ that coincide with the curves $J_c = J_c(L)$..

Indeed, such envelopes must satisfy Eqs. (A.6) and (A.7) along with the conditions

$$\frac{\partial(\mathcal{H}, \mathcal{J})}{\partial(k, \beta)} = 0 \tag{A.8}$$

and

$$\frac{\partial(\mathcal{H}, \mathcal{J})}{\partial(\alpha, k)} = 0, \tag{A.9}$$

respectively, where $\partial(\ldots)/\partial(\ldots)$ are Jacobians. However, by (A.3) and (A.4), both Eqs. (A.8) and (A.9) reduce to Eq. (23) that defines the boundaries of stability regions of ϕ_s and ϕ_p. This fact proves the identity $J_c \equiv J_{\max}$.

1. I.O. Kulik, *Zh. Eksp. Teor. Fiz.* **51**, 1952 (1966) [*Sov. Phys. JETP* **24**, 1307 (1967)].
2. B.D. Josephson, *Adv. Phys.* **14**, 419 (1965).
3. I.O. Kulik and I.K. Yanson, *The Josephson Effect in Superconductive Tunneling Structures*, Nauka, Moscow (1970) (in Russian).
4. L. Solymar, *Superconducting Tunneling and Applications*, Chapman and Hall, London (1972).
5. A. Barone and G. Paterno, *Physics and Applications of the Josephson Effect,* Wiley, New York (1982).

6. K.K. Likharev, *Dynamics of Josephson Junctions and Circuits*, Gordon and Breach, New York (1986).
7. Yu.S. Galperin and A.T. Filippov, *Zh. Eksp. Teor. Fiz.* **86**, 1527 (1984) [*Sov. Phys. JETP* **59**, 894 (1984)].
8. K.N. Yugay, N.V. Blinov, and I.V. Shirokov, *Phys. Rev*. **B49**, 12036 (1994); *Fiz. Nizk. Temp*. **25**, 712 (1999) [*Low Temp. Phys*. **25**, 530 (1999)].
9. E.G. Semerdjieva, T.L. Boyadjiev, and Yu.M. Shukrinov, *Fiz. Nizk. Temp*. **30**, 610 (2004) [*Low Temo. Phys*. **30**, 456 (2004)]; Yu.M. Shukrinov, E.G. Semerdjieva, and T.L. Boyadjiev, *J. Low Temp. Phys*. **139**, 299 (2005).
10. S.V. Kuplevakhsky and A.M. Glukhov, *Phys. Rev*. **B73**, 024513 (2006).
11. S.V. Kuplevakhsky and A.M. Glukhov, *Phys. Rev*. **B76**, 174515 (2007).
12. R.A. Ferrell and R.E. Prange, *Phys. Rev. Lett*. **10**, 479 (1963).
13. N.I. Akhiezer, *Elements of the Theory of Elliptic Functions*, Nauka, Moscow (1970) (in Russian).
14. R.K. Dodd, J.C. Eilbeck, J.D. Gibbon, and H.C. Morris, *Solitons and Nonlinear Wave Equations*, Academic Press, London (1982).
15. A.M. Kosevich and A.S. Kovalev, *An Introduction to Nonlinear Physical Mechanics*, Naukova Dumka, Kiev (1989) (in Russian).
16. Yu.M. Ivanchenko, A.V. Svidzinsky, and V.A. Slyusarev, *Zh. Eksp. Teor. Fiz.* **51**, 494 (1966) [*Sov. Phys. JETP* **24**, 131 (1967)].
17. C.S. Owen and D.J. Scalapino, *Phys. Rev*. **164**, 538 (1967).
18. R. Curant and D. Hilbert, *Methods of Mathematical Physics*, Interscience, New York (1962), Vol. II.
19. G. Jooss and D.D. Joseph, *Elementary Stability and Bifurcation Theory*, Springer, New York (1980).
20. J.M.T. Thompson, *Instabilities and Catastrophes in Science and Engineering*, Wiley, New York (1982).
21. From a mathematical point of view, it is by no means obvious that J_c thus defined should coincide with the parameter $J_{\max}$ that determines solvability of the problem (3)–(5): hence a necessity to prove the identity $J_c \equiv J_{\max}$ in Appendix A.
22. M. Abramowitz and I.A. Stegun, *Handbook of Mathematical Functions,* Dover, New York (1965).
23. S.V. Kuplevakhsky, *Phys. Rev*. **B60**, 7496 (1999); *ibid*. **63**, 054508 (2001).
24. E. Babaev, *Phys. Rev. Lett*. **89**, 067001 (2002).
25. R.G. Mints, I. Papiashvili, J.R. Kirtley, H. Hilgenkamp, G. Hammerl, and J. Mahnhart, *Phys. Rev. Lett*. **89**, 067004 (2002); R.G. Mints and I. Papiashvili, *Physica* **C403**, 240 (2004).
26. J.W. Bruce and P.G. Giblin, *Curves and Singularities,* University Press, Cambridge (1984).